Semi-empirical prediction of tone noise due to counter-rotating open rotors

Serge Lewy

ONERA, CFD and Aeroacoustics Department, MB 72, 92322 Chatillon, France

ABSTRACT

Counter-rotating open rotors (CROR) were extensively studied to power medium-size aircraft in the 80s after the first increases in fuel costs. Indeed, their efficiency is greater than that of turbofans and of single propfans. They have again become a topical subject due to the new increase of fuel costs and to the risk of oil shortage. They however raise a serious acoustic issue because noise is generated by the two rotors and by their interactions, and due to the lack of any shielding nacelle. An original and fast semi-empirical method is proposed to predict radiated sound levels. The objective is to rapidly assess if certification rules can be fulfilled, and to estimate the possible impact of a future fleet on noise contours around airports. This work is thus focused on takeoff and approach conditions (advancing Mach number lower than 0.3). It is shown that directivity of a tone is mainly determined by a Bessel function, and a parabolic pattern is suggested for overall sound pressure levels. The shape of third-octave spectra is based on the large number of interaction tones which are present in each frequency band. Finally, some information is given on overall sound levels.

INTRODUCTION

Emphasis was put on propfans during the 80s due to the first sudden rises in fuel costs [1]. They could power medium-haul airliners, with the advantage of having a better efficiency than turbofans (say, 80 percent instead of 65 percent) at nearly the same advancing Mach numbers ($M_{adv} \approx 0.7$ to 0.8). Efficiency is even higher if the swirling flow is recovered by an aft counter-rotating blade row (up to 10 percent additional fuel savings, see [1, Paper 12]). Several turboprops with counter-rotating propellers were thus designed, such as the Rolls-Royce project RB509 (diameter 3.90 m) [2] or the GE-36 Unducted fan (UDF®) of General Electric [3] which was tested in flight on a Boeing 727 (1986) and on a McDonnell-Douglas MD-80 (1988) – see Figure 1. Work on that subject decreased around 1990, partly due to the noise issue, but it knows a renewed interest for fear of depletion of oil stock and of new large increases in fuel costs.

Acoustics of counter-rotating open rotors (CROR) is a major issue because of the high tip speeds and of the interactions between the two blade rows. It is all the more noisy because there is no cowling to screen and absorb sound waves radiating towards the fuselage (comfort of passengers) or towards the ground (community annoyance). Moreover, pusher propellers are designed in most projects which require an upstream pylon generating another interaction with the rotating blades. A first analytical and experimental study (in static) was published by Hubbard in 1948 [4]. Hanson described the physics of noise generation [5], [6]. Parry and Crighton deduced simpler radiation equations at the limit of a large number of blades [7]. Peake and Boyd then suggested a transfer function for a fast calculation of near field starting from far-field approximation [8] (their work is pertinent to estimate cabin noise and also to extrapolate measurements in

non-anechoic wind tunnels). General Electric applied Hanson's equations on a previous model for single transonic propellers [9] to get an industrial method [10]. Now, CFD (Computational Fluid Dynamics) and CAA (Computational AeroAcoustics) begin to predict aerodynamics and acoustics of CROR at take-off conditions [11]. A hybrid method matching CFD and CAA has also been implemented at ONERA for counter-rotating ducted fans [12].

Source: Burkhard Domke, 2001
Figure 1. View of the General Electric UDF® mounted on a McDonnell-Douglas MD-80

The main concern is to fulfil the ICAO (International Civil Aviation Organization) certification rules. Present work is thus focused on low speed flight (i.e., $M_{adv} \approx 0.2$ to 0.3 in takeoff and approach conditions) such that the helical tip Mach number is subsonic. A fast semi-empirical computation of CROR tone noise is suggested to predict the effects of the main parameters, or to estimate the acoustic impact of aircraft traffic around airports. The key characteristics of the tones

are summarized in the next section. Following sections will present the results on directivity, third-octave spectra, and overall sound levels.

MAIN CHARACTERISTICS OF TONE NOISE

Radiating tones

The main parameters governing acoustic radiation are the number of blades in each rotor, B_1 and B_2, their tip speeds, and the blade loadings. Sound spectra are dominated by the harmonics of each blade passing frequency, $f_1 = |n_1 B_1 N_1|$ and $f_2 = |n_2 B_2 N_2|$, and by the interaction tones between the two rotors, at frequencies $f_{12} = |n_1 B_1 N_1 + n_2 B_2 N_2|$. In these equations, N_1 and N_2 are the rotation speeds, and n_1 and n_2 are positive or negative integers. The circumferential mode of a tone f_{12} is $m = n_2 B_2 - n_1 B_1$, the second row being taken as the reference of the rotation direction for the sign of m [5]. This generalizes the conventional formula $m = n_2 B_2 - n_1 V_1$ for $f_2 = |n_2 B_2 N_2|$ if the first row is fixed, i.e., is a stator ($N_1 = 0$ and $V_1 \equiv B_1$) [13].

The tip phase rotation Mach number, M_φ, of a wave (n_1, n_2) is a key parameter because radiation efficiency is large only at supersonic speeds $a M_\varphi$:

$$M_\varphi = \frac{2\pi f}{m} \cdot \frac{R}{a} = \frac{|n_1 B_1 N_1 + n_2 B_2 N_2|}{n_2 B_2 - n_1 B_1} \cdot \frac{2\pi R}{a} \qquad (1a)$$

or

$$M_\varphi \approx \frac{|n_2 B_2 + n_1 B_1|}{n_2 B_2 - n_1 B_1} M_{rot} \quad \text{if } N_1 \approx N_2, \qquad (1b)$$

where a is the speed of sound, R is the rotor radius (assumed to be approximately the same for the two rows), and $M_{rot} \approx 2\pi R N_2 / a$ is the tip rotational Mach number. The assumption $N_1 \approx N_2$ (Eq. 1b) is usually true. In practice, N_2 is often slightly lower than N_1 which provides a small acoustic gain (around 0.5 to 1 dB if N_2 is 10% lower and N_1 is 10% higher, according to [14]). On the contrary, reducing N_1 compared to N_2 would imply to increase blade loading in the first row to keep the same thrust, and therefore wake defect and interaction tones would also be increased [15].

Tones due to each rotor are such that $n_1 = 0$ or $n_2 = 0$, and $|M_\varphi| \approx M_{rot}$. They only radiate efficiently at cruise speed because the helical tip Mach number becomes supersonic. $|M_\varphi|$ is larger than M_{rot} if n_1 and n_2 have the same sign, and is much smaller than M_{rot} if n_1 and n_2 are of opposite sign. It is the reason why interaction tones are always sums $f_1 + f_2$ and never differences. For instance, fundamental frequencies are due to each rotor, i.e., $n_1 = 1$ and $n_2 = 0$ or $n_1 = 0$ and $n_2 = 1$, but neighbor interaction tones such as $n_1 = 2$ and $n_2 = -1$ or $n_2 = -3$ do not radiate [6]. As a consequence, absolute values in the above expressions for frequencies are useless, and it is sufficient to limit n_1 and n_2 to positive integers.

Special case

If the two rotors have the same number of blades and the same rotation speed ($B_1 = B_2 = B$ and $N_1 = N_2 = N$), the tone frequencies are $f = nBN$, where $n = n_1 + n_2$, and $m = (n - 2n_1)B$. Plane wave ($m = 0$) cannot be generated on odd-order harmonics but efficiently radiates around the axis (i.e., far upstream and far downstream) for even-order harmonics.

Also, orders n_1 and $n_1' = (n - n_1)$ generate modes $+m$ and $-m$ on any tone (n_1 and n_2 are inverted). A frequency $f = nBN$

contains two terms, in $\exp(+im\varphi)$ and in $\exp(-im\varphi)$ where φ is the circumferential angle (in the rotor plane) which creates a standing wave in $\cos(m\varphi)$. This was evidenced by Block who found differences of 10 dB between high and low overall sound pressure levels along angle φ [16]. The effect is stronger on odd harmonics because even harmonics are dominated by the plane wave $m = 0$.

DIRECTIVITY PATTERNS

Directivity of a tone

Sound pressure radiated on a tone of wave-number $k = 2\pi f / a$ and of mode m is governed by the Bessel function of first kind and of order m, $J_m(kR\sin\theta) = J_m(mM_\varphi \sin\theta)$, where θ is the angle in the horizontal plane ($\theta = 0$ on the upstream axis). It is confirmed that the argument is much lower than the order m if $|M_\varphi| \ll 1$ and the value of J_m is negligible. The above expression is valid if the microphone is linked to the aircraft (static or wind tunnel test). If it is fixed to the ground, frequencies are divided by $(1 - M_{adv}\cos\theta)$ due to the Doppler effect such that the Bessel function also depends on the advancing Mach number, M_{adv}:

$$J_m\left(\frac{kR\sin\theta}{1 - M_{adv}\cos\theta}\right). \qquad (2)$$

Distances (in the amplitude terms only but not in the phase terms) are multiplied by $(1 - M_{adv}\cos\theta)$.

For instance, directivity patterns radiated at the blade passing frequency of two counter-rotating eight-bladed rotors at the same rotation speed, $BPF = B_1 N_1 = B_2 N_2$, were measured in [17]. They are reproduced in Figure 2 (black triangles for flight test and black squares for model test). The Bessel function J_8, with $kR = 6.464$ (red dashed line with open symbols) is superimposed to the graph (the vertical position has been adjusted). It well duplicates the shape of the experimental data. Underprediction near the engine centerline (small and large angles) can be due to lower-order modes generated by the interaction between the upstream pylon and the first blade row [18].
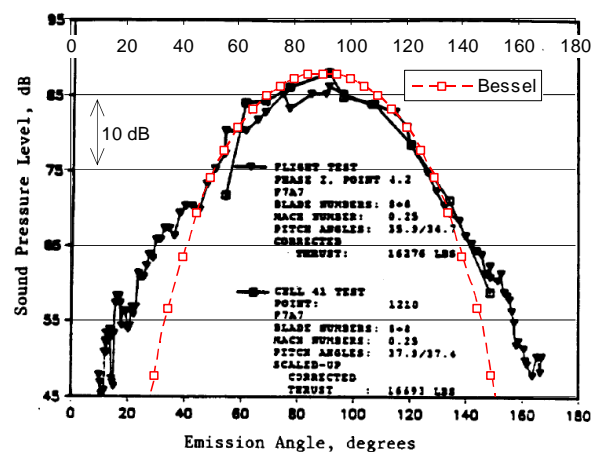

Source: Experimental data (flight test and model test)
from Figure 16(a) of [17]
Figure 2. Measured directivity of the blade passing frequency compared to the Bessel function.

Another example of measurements along a sideline at $M_{av} = 0.2$ is reproduced in Figure 3a, from [19]. Here, $B_1 = 11$, $B_2 = 9$, and $N_1 = N_2$. Figure 3b is a plot of the corresponding Bessel functions which are multiplied here by $\sin\theta$ to take into account the variation of distance. The

parameters are $m = B_1 = 11$ at $kR = 8.888$ for the blade passing frequency of the first row, BPF_1, $m = B_2 = 9$ at $kR = 7.272$ for BPF_2, $m = -2$ ($n_1 = n_2 = 1$) for the first interaction tone $BPF_1 + BPF_2$ at $kR = 16.16$. The shapes of these curves are in good agreement with the experiment of Figure 3a (note for instance the trough at 46° on $BPF_1 + BPF_2$ in the two graphs).
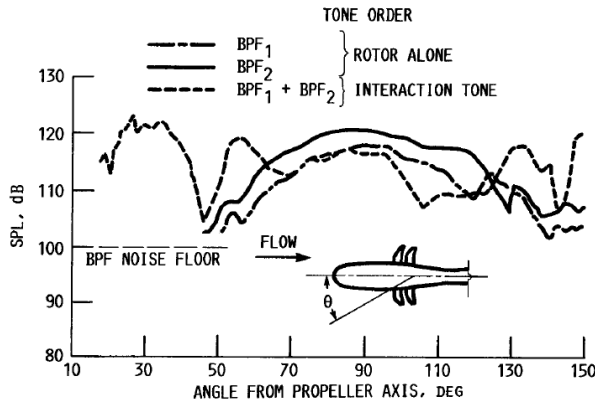
Source: From Figure 6 of [19]
a) Measurements along a sideline
(SPL = Sound pressure level)
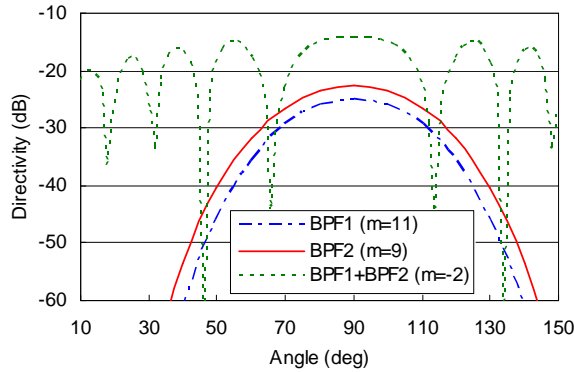
b) Directivities described by Bessel functions
Figure 3. Comparisons between directivity measurements and Bessel functions

As is explained in the previous section, tones due to each rotor can strongly radiate at cruise speed because helical tip speed is supersonic. They generally dominate the interaction tones, and they peak around 90 deg which is particularly annoying for passengers (Figure 2). The engines are thus put aft of the fuselage in most projects to reduce cabin noise (and also to save the pressurized cabin from any danger of blade separation).

In certification conditions at lower advancing speed (takeoff and approach), interaction tones are more important. Their Bessel functions are higher because they are of low order, and they extend far upstream and downstream (Figure 3). This is penalizing for EPNL (Effective Perceived Noise Level) integrated during the whole flight over. The two tones BPF_1 and BPF_2 generally remain noticeable even if $|M_\varphi| \approx M_{rot} < 1$ for two reasons: (i) They are generated by the blade steady loading which is much stronger than rotor-to-rotor interactions; (ii) The orders $m = B_1$ or B_2 of the Bessel functions are not too large. Higher harmonics do not usually exceed the broadband component: in the example of Figure 3, the maximum of the Bessel function at $2 \times BPF_2$, $J_{18}(14.544)$, gives a sound pressure level 9.6 dB lower than that at BPF_2, $J_9(7.272)$.

Directivity of overall sound pressure level

Several tests have shown that the overall directivity, Φ, in decibels can be approximated by a parabola with a maximum (taken equal to 0 dB) at $\theta = 90$ deg, such that:

$$\Phi(\theta) = -\alpha[\theta(\theta - 180) + 90^2] \text{ in dB,} \qquad (3a)$$

where θ is in degrees and α is a constant. A valid estimate seems to be $\alpha \approx 0.002$. Directivity on a sideline is useful to compute EPNL:

$$\Phi'(\theta) = \Phi(\theta) + 20 \log_{10}(\sin\theta). \qquad (3b)$$

The two curves (3a) and (3b) are plotted in Figure 4 with $\alpha = 0.002$. It is assessed in Figure 5 that the directivity along a sideline (dashed line in Figure 4) well compares with measurements published in [20] (the vertical position of the predicted curve is arbitrary).
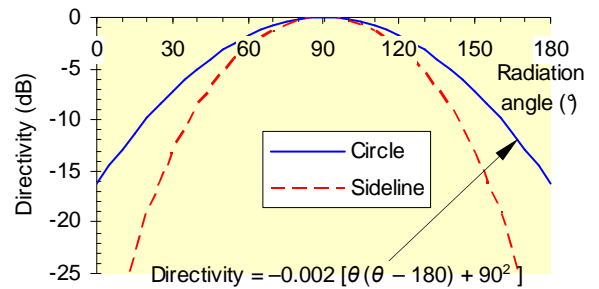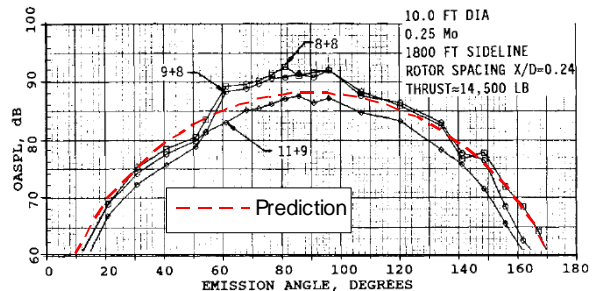

Figure 4. Analytical directivity for overall sound pressure level

Source: Experimental data from Figure 7(a) of [20]
Figure 5. Comparison of the predicted directivity with measurements of overall sound pressure level, OASPL, along a sideline

THIRD-OCTAVE SPECTRA

Number of tones in a third-octave band

Interaction tones f_{12} between the two rotors are very numerous, and there are several tones in each third-octave band as soon as their central frequencies, f_c, are not too low. As the bandwidth is proportional to f_c, the number of tones due to each rotor is roughly proportional to f_c in a band, and the number of tones, n_{tot}, due to the two rotors is roughly proportional to $(f_c)^2$.

This is shown in Figure 6 (red solid line with open symbols) for the full-scale configuration corresponding to Figure 3a (the scale of the model in [19], of diameter 62 cm, is approximately 1/5). It has been written about Eqs. (1a) and (1b) that only the waves with a supersonic phase Mach number, M_φ, efficiently radiate. Their number, n_{rad}, is also plotted in Figure 6 (blue dashed line with dark symbols), it is proportional to the total number, n_{tot}, and the ratio between the two numbers (supersonic phase speed and total) is here

approximately equal to 0.7 (mixed line with crosses, scale on the right hand side of Figure 6).

This ratio, n_{rad}/n_{tot}, increases of course with M_{rot} (see Eq. 1b). Figure 7 shows that it is approximately equal to M_{rot}:

$$n_{rad}/n_{tot} \approx M_{rot}. \tag{4}$$

As it is also evident from Figure 7, there are less and less tones in the range of third-octave bands from 25 Hz to 20 kHz when M_{rot} increases because the blade passing frequencies increase with M_{rot}. However, all the tones tend to radiate if M_{rot} approaches 1 (Figure 6 corresponds to $M_{rot} = 0.72$).
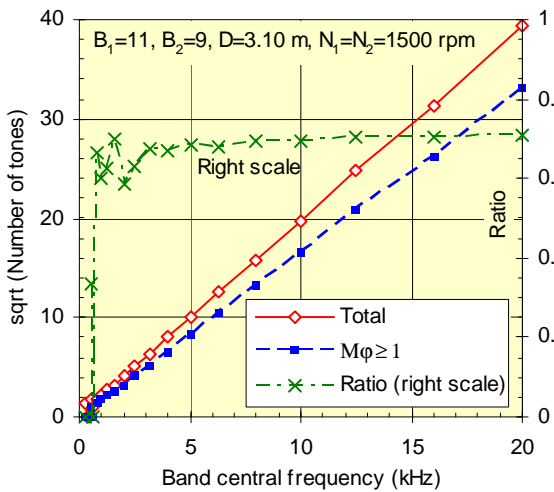

Figure 6. Square root of the number of tones in third-octave bands
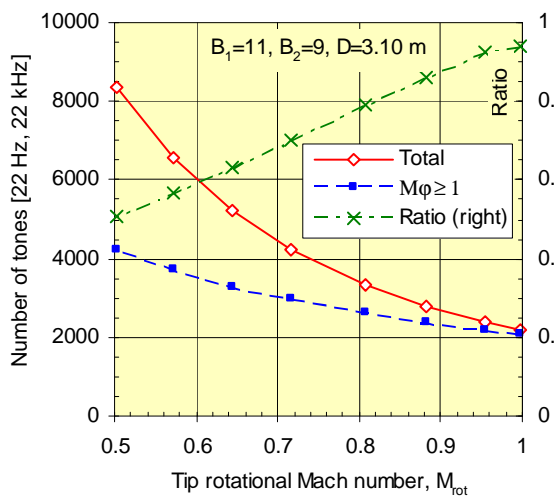

Figure 7. Number of tones in the whole acoustic range versus tip rotational Mach number

Model of third-octave spectrum

It is seen in Figure 6 that the number of tones in each third-octave band is rather large as soon as the frequency is not very low. The same kind of argument as density of modes in room acoustics is thus suggested here. According to various experimental results, third-octave spectra decrease of about 10 dB per octave in the high frequency range, which means a slope of the squared sound pressure in $(1/f)^3$. This shape is duplicated in the prediction if the amplitude of each tone is proportional to $(1/f)^5$ in case of $(n_1 + n_2) > 5$. The amplitudes are assumed to remain constant if $(n_1 + n_2) \leq 5$ to avoid that they become very large at low frequency.

This leads to the predictions of Figure 8 for three pairs (B_1, B_2). The solid line with dark symbols corresponds to the full-scale configuration equivalent to [19] (from NASA) or [20] (from General Electric). The case $B_1 = 9$, $B_2 = 8$ was also tested in [20]. The absolute sound pressure levels will be discussed at the end of the sub-section "General formulae" in the next section.

Two comments can be made. Firstly, Parry computed the sound power spectrum of the tones due to blade row interaction and found that the result strongly depended on the wake model [7], [21]. Secondly, the low frequency part of the spectra in Figure 8 would be filled up with the broadband component. A semi-empirical model has been recently proposed to predict the interaction between turbulent rotor wakes and a rear rotor, but levels are much lower than measurements, and other noise sources are suspected to dominate [22].
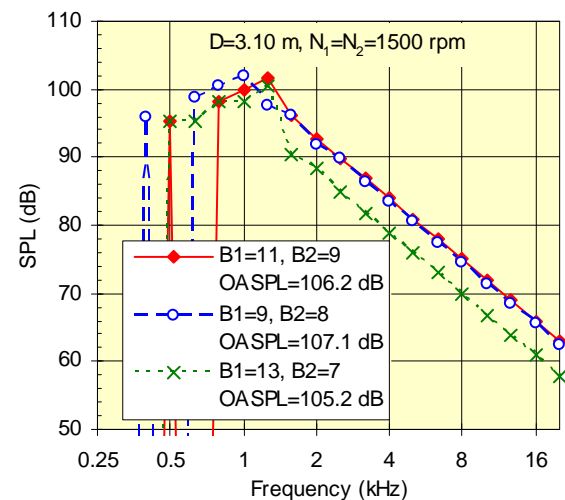

Figure 8. Shape of the predicted third-octave spectrum due to the interaction tones (OASPL = Overall sound pressure level)

Figure 9 is a 3D view of sound pressure level versus third-octave bands and radiation angle, for the same conditions as the solid line (red curve) in Figure 8. The two blade passing frequencies, BPF_1 (275 Hz) and BPF_2 (225 Hz), are included in this figure, according to the comment at the end of the sub-section "Directivity of a tone". They both lie in the 250 Hz third-octave band, and their directivity patterns are in Bessel functions.
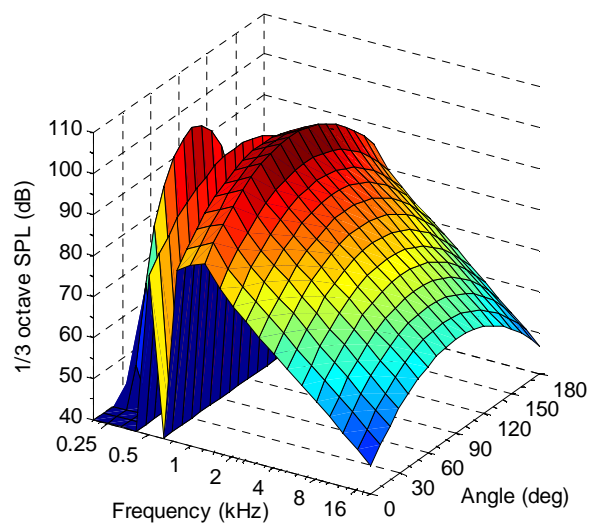

Figure 9. Sound pressure level versus third-octave bands and radiation angle: $B_1 = 11$, $B_2 = 9$, $D = 3.10$ m, and $N_1 = N_2 = 1500$ rpm

ABSOLUTE SOUND LEVELS

General formulae

Experimental results show that overall sound levels generated by a given CROR mainly depend on the thrust, T, whatever may be the combinations between rotation speed, blade angle of attack, and advancing speed. If U_{adv} is the advancing speed ($U_{adv} = aM_{adv}$) and U_e the CROR exit velocity:

$$T = \frac{1}{2}\rho_0(\pi R^2)(U_e^2 - U_{adv}^2), \tag{5a}$$

where ρ_0 is the air density. The velocities are proportional to aM_{rot} or $2\pi RN$ if $N_1 \approx N_2 \approx N$, and T can also be written:

$$T = C_T \rho_0 N^2 D^4, \tag{5b}$$

where $D = 2R$ is the diameter and C_T is the thrust coefficient (generally lower than 0.3). Noise generation is mainly of dipole type, and thus varies as N^6. Finally, overall sound pressure level, OASPL, is in decibels:

$$\text{OASPL} = 30\log_{10}T - 20\log_{10}r + \Phi(\theta) + C, \tag{6}$$

where r is the distance in meters and C is a constant. This leads to the overall sound power level, OAPWL, for an axisymmetric radiation (without angular standing waves, see the end of the section on the "Main characteristics"):

$$\text{OAPWL} = 30\log_{10}T + 8.9 \text{ dB} + C \tag{7}$$

for $\alpha = 0.002$ in Eq. (3a). This can be used to estimate the constant C (the same in Eqs. 6 and 7), assuming an "acoustic efficiency", ratio between acoustic power, W_{ac}, and shaft mechanical power, W_{mec}. More precisely, W_{ac} depends on $(W_{mec}/D^2)/B_{tot}$, where $B_{tot} = B_1 + B_2$. Indeed, the sound pressure levels measured in [23] and [20] for several pairs (B_1, B_2) collapse on a single curve versus thrust per blade or power per blade. Also note that the value (W_{mec}/D^2) has to be the same at full scale and for model tests. The above relation means that the constant C, valid for values B_{tot} and D, becomes C' for other values B'_{tot} and D', such that:

$$C' = C - 20\log_{10}(D'/D) - 10\log_{10}(B'_{tot}/B_{tot}). \tag{8}$$

This also tends to indicate that it is beneficial to take a larger diameter and to increase the numbers of blades, keeping the same tip speed.

Spectra of Figure 8 are computed at the maximum of sound pressure (i.e., for $\theta = 90$ deg) at a distance $r = 100$ m. The OASPL are written in the legend of that figure. It is checked that OASPL is slightly lower if the total number of blades, B_{tot}, is higher. It is also noticed that it is better to have a greater difference between B_1 and B_2 for a given total number of blades, B_{tot}.

Some corrections

The correction found in Ref. [8] increases the sound levels in the near field but becomes negligible at two rotor diameters. However, sound pressure increases exponentially if distance decreases when M_{φ} is subsonic (similar to evanescent waves in a duct).

The distance ℓ between the two rows has of course nearly no effect on the tones due to each propeller. For the interaction tones, Dittmar suggested in [24] a variation of sound pressure level in $-20\log[(\ell/c_1) + 0.3]$ for the effect of the wakes shed from the forward row, and in $-10\log(\ell/c_1)$ for the effect of the tip vortices, where c_1 is the chord of the front blades (Figure 10).

Tip vortex interaction noise seems to be predominant but its prediction still requires relevant studies [25]. Moreover, it decreases more slowly than the wake interaction term (Figure 10), and some tests were made with clipped aft blades to avoid interactions with upstream vortices [26], [20]. Block *et al.* also tested a rear rotor with a reduced diameter but they did not find any effect [23]; they noticed that they used straight blades, and the noise due to wake encounter was probably high in that case.
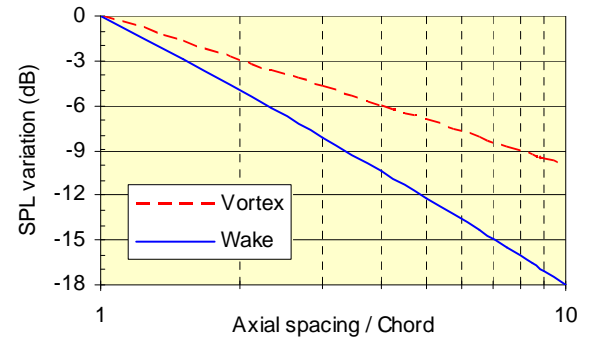

Figure 10. Effect of the spacing between the two rotors on sound pressure levels, according to [24]

Finally, if it is assumed that constant C is valid for a basic configuration (tractor propellers at 0-deg angle of attack), some modifications can be made according to the synthesis of Magliozzi [27]. They are given in Table 1. Pusher propellers require an upstream pylon which can increase the front rotor BPF by more than 10 dB, but its effect is negligible on interaction tones [28]. It is why the corrections on overall sound levels are comparatively small. Also note that the correction for pusher propellers with an angle of attack is lower than the sum of the two other values (1.5 dB and 3.5 dB). In fact, tests of [19] have shown that an angle of attack increases the rotor-alone tones (BPF_1 and BPF_2) but has not a strong influence on interaction tones.

Table 1. Corrections on overall sound levels due to the configuration

CROR	Angle of attack	
	Zero degree	Non-zero
Tractor	Reference = 0 dB	+3.5 dB
Pusher	+1.5 dB	+2.5 dB

CONCLUSIONS

Noise radiation of counter-rotating open rotors can impede their expansion in medium-size aircraft due to the interactions between the two blade rows and to the absence of cowling around them which could absorb a part of the acoustic waves. This work suggests a fast computation of directivity and spectral shape of the tones. The main originality lies in the way of computing third-octave spectra, on the basis of the number of tones in each frequency band. There is also a broadband component which mainly completes the spectra in the low frequency range, but it should not change too much the overall sound levels (this is specially true in weighted decibels which attenuate low frequencies).

The interest of the method is twofold. Firstly, it can be assessed if a future aircraft will fulfill the certification rules. Secondly, the annoyance due to a new fleet equipped with counter-rotating open rotors around the airport area can be

estimated. Such a semi-empirical approach is all the more useful because recent publications (e.g., see [11], [22], [25]) and studies at ONERA (see [12]) show that analytical and numerical acoustic predictions of counter-rotating rotors remain a challenge which is in progress.

ACKNOWLEDGEMENTS

REFERENCES

1   *Aerodynamics and acoustics of propellers*, AGARD CP-366 (1985)

2   T.J. Kirker, *Procurement and testing of a 1/5 scale advanced counter rotating propfan model*, AIAA Paper 90-3975, AIAA 13th Aeroacoustics Conference, Tallahassee, FL (1990)

3   J.B. Taylor, *Unducted, counterrotating gearless front fan engine*, U.S. Patent No. 4,976,102 (1990)

4   H.H. Hubbard, *Sound from dual-rotating and multiple single-rotating propellers*, NACA TN-1654 (1948)

5   D.B. Hanson, "Noise of counter-rotation propellers" AIAA Paper 84-2305 & *J. Aircraft* **22**, 609-617 (1985).

6   D.B. Hanson and C.J. McColgan, "Noise of counter-rotation propellers with nonsynchronous rotors" *J. Aircraft* **22**, 1097-1099 (1985)

7   A.B. Parry and D.G. Crighton, *Prediction of counter-rotation propeller noise*, AIAA Paper 89-1141, AIAA 12th Aeroacoustics Conference, San Antonio, TX (1989)

8   N. Peake and W.K. Boyd, "Approximate method for the prediction of propeller noise near-field effects" AIAA Paper 90-3998 & *J. Aircraft* **30**, 603-610 (1993)

9   C.E. Whitfield, P.R. Gliebe, R. Mani, and P. Mungur, *High speed turboprop aeroacoustic study – Single rotation. Volume I – Model development*, NASA CR-182257 (1989)

10 C.E. Whitfield, R. Mani, and P.R. Gliebe, *High speed turboprop aeroacoustic study (counterrotation), Vol. I – Model development; Vol. II – Computer programs*, NASA CR-185241 & CR-185242 (1990)

11 A. Stuermer and J. Yin, *Low-speed aerodynamics and aeroacoustics of CROR propulsion systems*, AIAA Paper 2009-3134, 15th AIAA/CEAS Aeroacoustics Conference, Miami, FL (2009)

12 C. Polacsek, R. Barrier, *Numerical simulation of counter-rotating fan aeroacoustics*, AIAA Paper 2007-3680, 13th AIAA/CEAS Aeroacoustics Conference, Rome, Italy (2007)

13 J.M. Tyler and T.G. Sofrin, "Axial flow compressor noise studies" *Society of Automotive Engineers (SAE) Transactions* **70**, 309-332 (1962)

14 B. Magliozzi, P. Brown, and D. Parzych, *Acoustic test and analysis of a counterrotating prop-fan model*, NASA CR-179590 (1987)

15 R.P. Woodward and C.E. Hughes, *Aeroacoustic effects of reduced aft tip speed at constant thrust for a model counterrotation turboprop at takeoff conditions*, AIAA Paper 90-3933, AIAA 13th Aeroacoustics Conference, Tallahassee, FL (1990)

16 P.J.W. Block, "Noise radiation patterns of counter-rotation and unsteadily loaded single-rotation propellers" AIAA Paper 84-2263 & *J. Aircraft* **22**, 776-783 (1985)

17 G.E. Hoff et al., *Experimental performance and acoustic investigation of modern, counterrotating blade concepts*, NASA CR-185158 (1990)

18 C.E. Whitfield and P.R. Gliebe, *Predicted vs. scale model and flight test UDF® engine noise*, AIAA Paper 90-3936, AIAA 13th Aeroacoustics Conference, Tallahassee, FL (1990)

19 R.P. Woodward, *Noise of a model high-speed counterrotation propeller at simulated takeoff/approach conditions (F7/A7)*, AIAA Paper 87-2657, AIAA 11th Aeroacoustics Conference, Sunnyvale, CA (1987)

20 B.A. Janardan and P.R. Gliebe, "Acoustic characteristics of counterrotating unducted fans from model scale tests" AIAA Paper 89-1142 & *J. Aircraft* **27**, 268-275 (1990)

21 A.B. Parry, "Modular prediction scheme for blade row interaction noise" *J. Propulsion and Power* **13**, 334-341 (1997)

22 V.P. Blandeau, P.F. Joseph, and B.J. Tester, *Broadband noise prediction from rotor-wake interaction in contra-rotating propfans*, AIAA Paper 2009-3137, 15th AIAA/CEAS Aeroacoustics Conference, Miami, FL (2009)

23 P.J.W. Block, R.J. Klatte, and P.M. Druez, *Counter-rotating propeller noise directivity and trends*, AIAA Paper 86-1927, AIAA 10th Aeroacoustics Conference, Seattle, WA (1986)

24 J.H. Dittmar, *Some design philosophy for reducing the community noise of advanced counter-rotation propellers*, NASA TM-87099 (1985)

25 M.J. Kingan and R.H. Self, *Counter-rotation propeller tip vortex interaction noise*, AIAA Paper 2009-3135, 15th AIAA/CEAS Aeroacoustics Conference, Miami, FL (2009)

26 R.P. Woodward and E.B. Gordon, *Noise of a model counterrotation propeller with reduced aft rotor diameter and simulated takeoff/approach conditions (F7/A3)*, AIAA Paper 88-0263, AIAA 26th Aerospace Sciences Meeting, Reno, NV (1988)

27 B. Magliozzi, *Noise characteristics of model counter-rotating prop-fans*, AIAA Paper 87-2656, AIAA 11th Aeroacoustics Conference, Palo Alto, CA (1987)

28 B.N. Shivashankara, D.P. Johnson, and R.D. Cuthbertson, *Installation effects on counter rotating propeller noise*, AIAA Paper 90-4023, AIAA 13th Aeroacoustics Conference, Tallahassee, FL (1990)